

Solvent- and Light-Controlled Unidirectional Transit of a Nonsymmetric Molecular Axle Through a Nonsymmetric Molecular Wheel

Arturo Arduini,^{*,[a]} Rocco Bussolati,^[a] Alberto Credi,^{*,[b]} Simone Monaco,^[b]
Andrea Secchi,^[a] Serena Silvi,^[b] and Margherita Venturi^{*,[b]}

Abstract: The development of a pseudorotaxane motif capable of performing unidirectional threading and dethreading processes under control of external stimuli is particularly important for the construction of processive linear motors based on rotaxanes and, at least in principle, it discloses the possibility to access to rotary motors based on catenanes. Here, we report a strategy to obtain the solvent-controlled unidirectional transit of a molecular axle through a molecular wheel. It is based on the use of appropriately designed molecular components, the essential feature of which is their non-

symmetric structure. Specifically they are an axle containing a central electron-acceptor 4,4'-bipyridinium core functionalized with a hexanol chain at one side, and a stilbene unit connected through a C6 chain at the other side, and a heteroditopic tris(phenylureido)-calix[6]arene wheel. In apolar solvents the axle threads into the wheel from its upper rim and with the end carrying the OH group, giving an oriented pseu-

dorotaxane structure. After a stopping reaction, which replaces the small hydroxy group with a bulky diphenylacetyl moiety, and replacement of the apolar solvent with a polar one, dethreading occurs through the slippage of the stilbene unit from the lower rim of the wheel, that is, in the same direction of the threading process. The essential role played by the stilbene unit to achieve the unidirectional transit of the axle through the wheel, and to tune the dethreading rate by light is also demonstrated.

Keywords: calixarenes • pseudorotaxanes • supramolecular chemistry • unidirectional transit • viologens

Introduction

The principles and methods of supramolecular chemistry applied to the construction of working devices and molecular machines represent a powerful strategy for the development of nanoscience and nanotechnology as well as for the comprehension of the several biological processes in which natural motors and machines operate.^[1-5] Pseudorotaxanes, supramolecular complexes minimally composed of a wheel-type host surrounding an axle-type guest,^[6,7] are the simplest prototypes of artificial molecular level machines.^[8] Their working mechanism is based on the assembly/disassembly of the axle and the wheel components and it resembles the threading/dethreading of a needle. The fact that these move-

ments can be controlled by external stimulation^[8,9] makes such systems appealing for the development of functional materials.^[10,11] Furthermore, studies on switchable pseudorotaxanes^[12-17] are of great interest for the development of molecular machines based on rotaxanes, catenanes, and related interlocked compounds. Specifically, the development of a pseudorotaxane motif capable of performing unidirectional threading and dethreading processes^[18-25] under the control of external stimuli (Figure 1 a) would be important for the

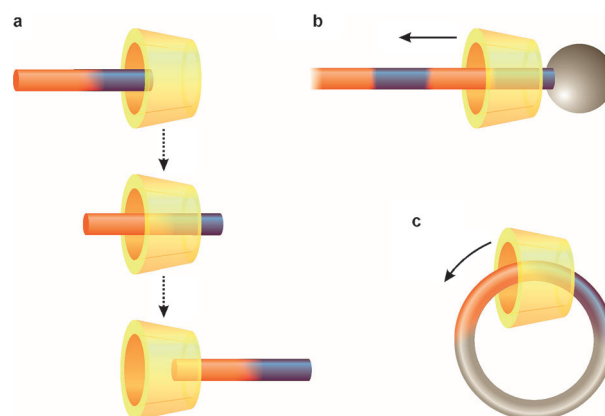


Figure 1. Representation of unidirectional threading/dethreading of a [2]pseudorotaxane with a) nonsymmetric components, b) a processive linear motor based on a [2]rotaxane, and c) a rotary motor based on a [2]catenane.

[a] Prof. A. Arduini, Dr. R. Bussolati, Prof. A. Secchi
Dipartimento di Chimica Organica e Industriale
Università degli Studi di Parma
Parco Area delle Scienze 17 A, 43124, Parma (Italy)
Fax: (+39)0521905472
E-mail: arturo.arduini@unipr.it

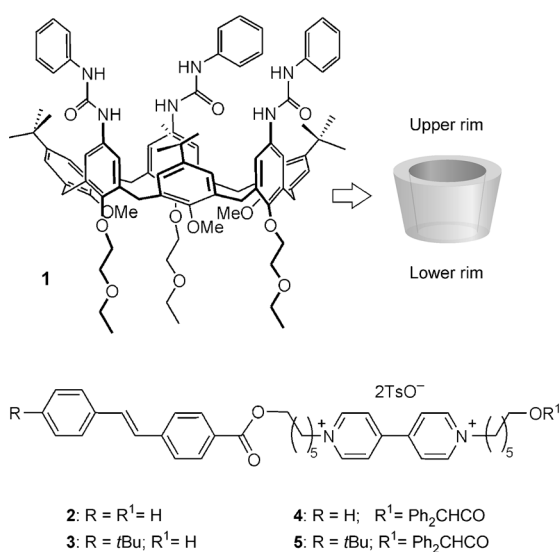
[b] Prof. A. Credi, S. Monaco, Dr. S. Silvi, Prof. M. Venturi
Dipartimento di Chimica "G. Ciamician"
Università di Bologna, Via Selmi 2, 40126 Bologna (Italy)
Fax: (+39)0512099456
E-mail: alberto.credi@unibo.it
margherita.venturi@unibo.it

Supporting information for this article is available on the WWW under <http://dx.doi.org/10.1002/chem.201201625>.

construction of processive linear motors based on rotaxanes (Figure 1b) and, at least as a perspective, for rotary motors based on catenanes (Figure 1c).^[26–28]

The essential feature of molecular motors is indeed the directional control of the motion, which is achieved by modulating not only the thermodynamics but also the kinetics of the transition between the mechanical states of the device. This result can be achieved by applying ratcheting concepts to the design of the systems.^[26–30] Although a few examples of artificial molecular rotary motors and DNA-based linear motors^[31–34] have been described, only one prototype of a fully synthetic linear motor molecule is available.^[35] This system, which is not based on a rotaxane, consists of a small molecular fragment that can “walk” progressively along a molecular “track” and its operation relies on a rather complex sequence of chemical reactions. Therefore, the construction of linear supramolecular motors is still an open problem and an important challenge, because linear movements are essential both in Nature and technology. In living organisms movements related to intracellular trafficking and muscle contraction are produced by linear motor proteins such as kinesin, dynein, and myosin;^[36] similarly, RNA polymerase moves along DNA while carrying out transcriptions.^[2] Indeed, biological supramolecular architectures are themselves the premier, proven examples of the feasibility and utility of nanotechnology, and constitute a sound rationale for attempting the realization of artificial nanomachines.^[1]

We recently demonstrated^[37–41] that the use of the heteroditopic nonsymmetric tris(phenylureido)calix[6]arene derivative **1** (Scheme 1) as a three-dimensional macrocyclic component^[42] for obtaining oriented pseudorotaxanes and rotaxanes brings about a significant increase in structural complexity because, in principle, it is possible to selectively address the threading of suitable axles from its “upper” or “lower” rim leading to “up” and “down” oriented isomers



Scheme 1.

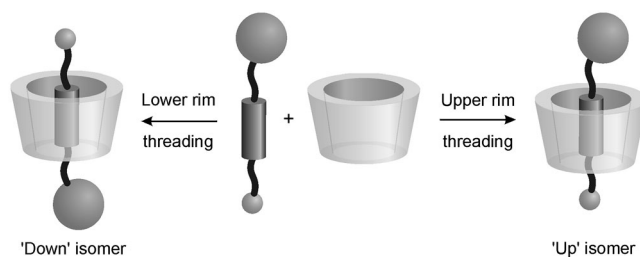


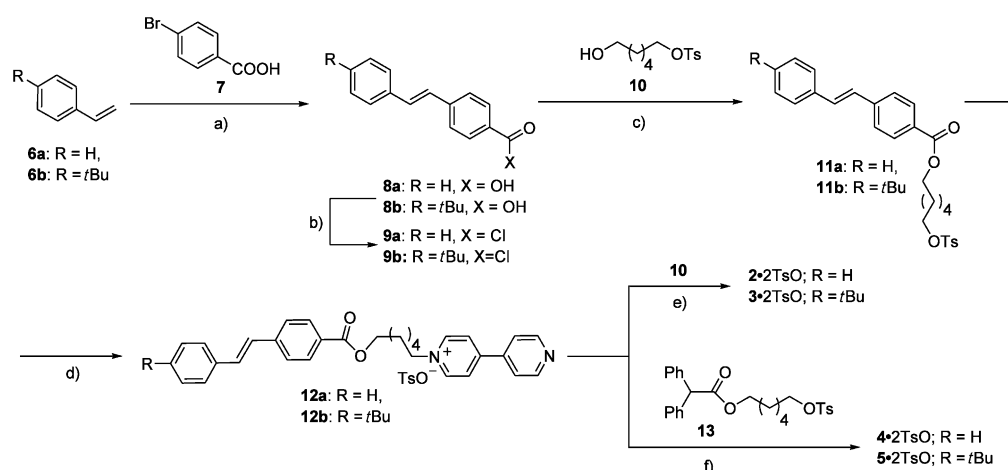
Figure 2. Formation of “up” and “down” orientated pseudorotaxane isomers by self-assembly of the nonsymmetric wheel and axle components.

(Figure 2). In fact, we showed that in apolar media (e.g., benzene) compound **1** is able to act as a very efficient^[38] wheel that can be threaded exclusively from the upper rim by axles derived from 4,4'-bipyridinium salts to yield oriented pseudorotaxanes.^[37,39] This behavior was explained by analyzing the main chemical and structural features of compound **1** as a host, which are 1) a π -donor macrocyclic cavity that, because of its width, can include the positively charged bipyridinium unit of the axle, but not together with its counter anions, 2) three efficient hydrogen-bonding donor ureidic groups at the upper rim that, by complexing the counter anions of the axle, can assist the insertion of the cationic portion of the latter into the cavity from this rim, and 3) three methoxy groups at the lower rim that, in apolar media, are oriented towards the interior of the cavity in the NMR timescale,^[43] thereby hindering the access of the guest from this direction. The use of a more polar solvent has a profound effect. In fact, the solvent polarity affects both the concentration of the active guest available in solution and the binding ability of the wheel, by changing the extent of ion pairing of the axle and decreasing the pivoting role of the three ureidic groups of the host, respectively.

Herein, we report a study in which the unidirectional transit of a molecular axle through wheel **1** is clearly demonstrated; the experimental results show indeed that the threading of the axle occurs from the upper rim of the wheel, and that the subsequent solvent-controlled dethreading takes place from the lower rim of the wheel, that is, in the same direction as the threading (Figure 1a).

Results and Discussion

Design and synthesis: To obtain pseudorotaxane systems based on wheel **1** capable of undergoing unidirectional threading/dethreading motion, the axles **2** and **3** as tosylate salts have been synthesized (see Scheme 2 and the Experimental Section). They are composed by a central electron-acceptor 4,4'-bipyridinium core functionalized with an hexanol chain at one side, and a stilbene (**2**) or a *t*Bu-substituted stilbene (**3**) unit connected through a C6 chain at the other side (Scheme 1). The terminal OH group was incorporated because it is easily involved in stopping reactions, whereas the stilbene and the *t*Bu -substituted stilbene head groups

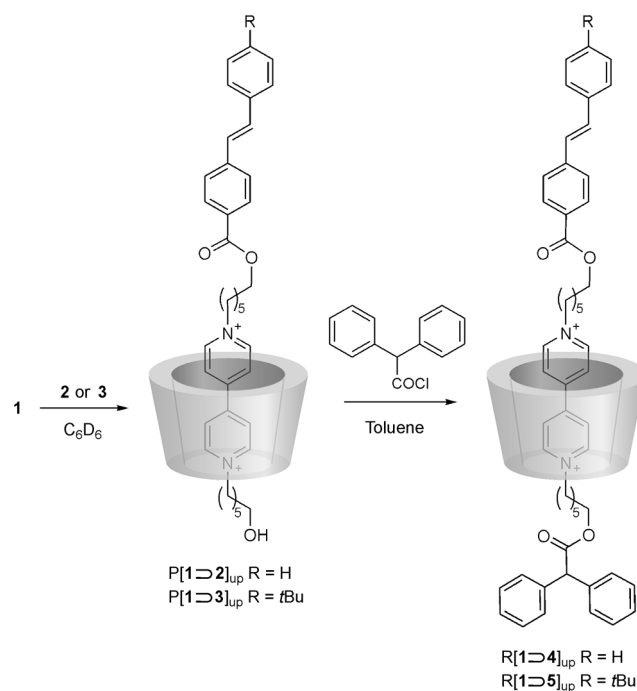


Scheme 2. Reagents and conditions: a) Pd(OAc)₂, K₂CO₃, *N,N*-dimethyl-β-alanine, DMF, heating to reflux, 6 h; b) oxalyl chloride, CHCl₃, heating to reflux, 2 h; c) NEt₃, 4-dimethylaminopyridine (DMAP), CH₂Cl₂, 48 h; d) 4,4'-bipyridine, CH₃CN, heating to reflux, 72 h; e) CH₃CN, heating to reflux, 15 h; f) CH₃CN, heating to reflux, 15 h.

were selected because 1) their dimensions are not too big to prevent their slippage^[44,45] through wheel **1**, but large enough to enable a kinetic control of the threading/de-threading of the axles in the wheel, as molecular mechanics calculations indicate,^[46] and 2) their capability to undergo *E-Z* photoisomerization with a consequent change in structure and hampering effect^[47–49] that can be exploited as a further element to kinetically control the threading/de-threading movements.^[50] For comparison purposes axles **4–5** were also synthesized (Scheme 2).

To verify the hypothesis that the stilbene-type head group of the synthesized axles can act as a kinetic control element during the threading process, wheel **1** and an excess of axle **2** or **3** were equilibrated in C₆D₆ at room temperature in separate experiments (Scheme 3). A red solution was obtained in both cases and, after removal of the excess of the axle, a full NMR analysis was performed.

As expected, the threading of axles **2** or **3** into the wheel results in a substantial rearrangement of the calix[6]arene skeleton; for example a downfield shift of about 1.1 ppm of the methoxy groups and the appearance of the AX system of two doublets experienced by the six pseudo-axial and the six pseudo-equatorial protons of the methylene bridges are clearly evidenced.^[37,39] In addition, the six ureido NH protons, because of their involvement in hydrogen bonding with the two tosylate anions, are shifted downfield of about 3 ppm. The inclusion inside the wheel also affects the resonances of axles **2** and **3**. The NMR signals of both compounds **2** and **3** in the pseudorotaxanes (Figure 3) are fully assigned through 1D and 2D NMR experiments (Figures S5–S13 in the Supporting Information). In particular, the aromatic protons of the 4,4'-bipyridinium core originate four doublets denoted as (7), (7'), (8), and (8') centered in both pseudorotaxane complexes at $\delta = 8.1$, 6.9, 7.9, and 6.8 ppm, respectively. As reported in previous studies,^[37,39] the presence of only two pairs of coupled doublets indicates that the axles have effectively threaded the wheel, because



Scheme 3. Self-assembly of P[**1**>**2**]_{up} and P[**1**>**3**]_{up}, and synthesis of R[**1**>**4**]_{up} and R[**1**>**5**]_{up}.

the protons of the two pyridinium moieties experience an asymmetrical magnetic environment due to their embedding into the truncated cone shape of the calix[6]arene macrocycle. Moreover 2D TOCSY experiments evidence the presence of only one set of signals for the two alkyl chains linked to the 4,4'-bipyridinium core in both pseudorotaxanes (Figures S7 and S11 in the Supporting Information). These findings suggest that one pseudorotaxane-type complex does form predominantly in a benzene solution. 2D ROESY NMR experiments (Figures S8, S12, and S13 in the Support-

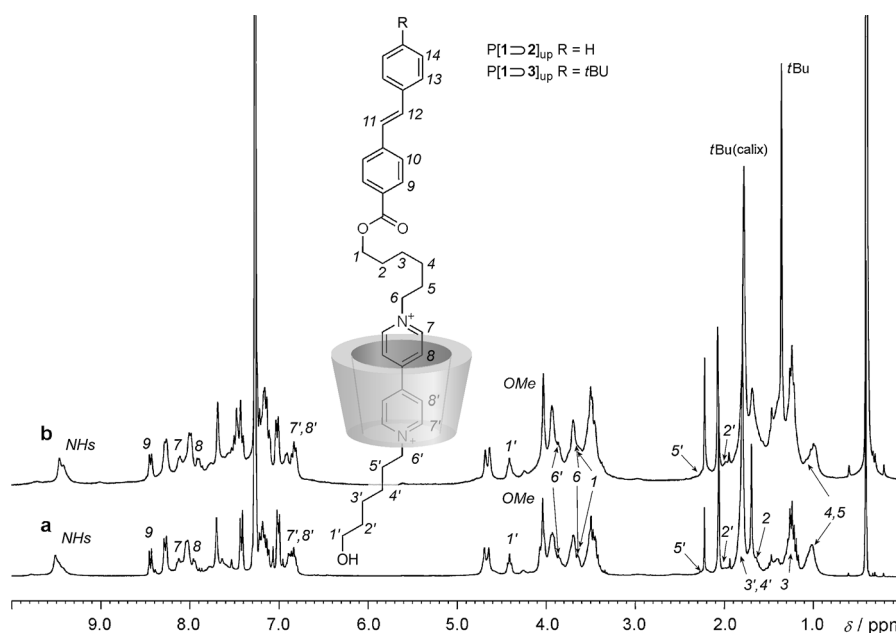


Figure 3. ^1H NMR spectra (300 MHz, C_6D_6) of different pseudorotaxanes: a) $\text{P}[\mathbf{1}\text{D}2]_{\text{up}}$ and b) $\text{P}[\mathbf{1}\text{D}3]_{\text{up}}$. The most diagnostic resonances of axles **2** and **3** have been numbered according to the pseudorotaxane sketch placed above the spectra (resonances of **1** have not been labeled for clarity, for further NMR characterizations see Figures S5–S13 in the Supporting Information).

ing Information) finally confirm that the stilbene-based head group of axles **2** and **3** is positioned at the upper rim of the wheel in both pseudorotaxanes thereby suggesting that both axles enter the wheel through the calixarene upper rim with their OH terminus to give the oriented species $\text{P}[\mathbf{1}\text{D}2]_{\text{up}}$ and $\text{P}[\mathbf{1}\text{D}3]_{\text{up}}$ (Scheme 3). This strict orientational control during the formation of the pseudorotaxane can be explained on the basis of the structural features of both the wheel^[40] and the axle. In fact, at least in principle, axles **2** and **3** could enter the wheel from its upper rim either through the OH or the stilbene terminus. The fact that under these experimental conditions only one orientational pseudorotaxane isomer is formed clearly indicates that the wheel pivots the threading of the axles from the upper rim and that the latter components access the macrocycle through the less bulkier OH terminus in a process that is kinetically controlled by the different size of the end groups of the axles (for a simplified energy diagram describing the possible threading modes see Figure S27 in the Supporting Information). This also means that, in agreement with our expectations, the presence of the stilbene-type units enables the kinetic control of the threading process, leading to the formation of the oriented pseudorotaxanes $\text{P}[\mathbf{1}\text{D}2]_{\text{up}}$ and $\text{P}[\mathbf{1}\text{D}3]_{\text{up}}$ (Scheme 3). These pseudorotaxane structures, as already evidenced for similar species,^[51] are stabilized by a variety of interactions, including 1) charge-transfer (CT) interactions between the π -electron-accepting 4,4'-bipyridinium unit incorporated in the axles and the π -electron-rich aromatic cavity of the wheel, which are responsible of the red color of the solution, 2) $\text{C}-\text{H}\cdots\pi$ interactions, 3) $\text{C}-\text{H}\cdots\text{O}$

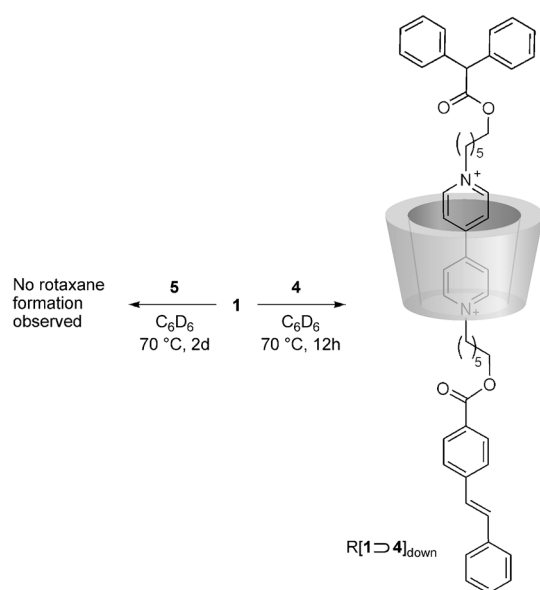
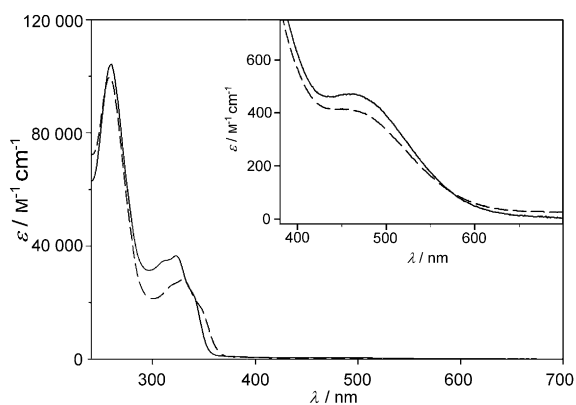
hydrogen bonds, and 4) hydrogen bonding between the counter anions of the axles and the ureidic NH fragments of the wheel.

To determine their stability constants, titrations of axles **2** and **3** with wheel **1** have been performed in CH_2Cl_2 at room temperature. In both cases, upon addition of the wheel to a solution of the axle the absorption features in the $\lambda=320$ – 600 nm spectral region, characteristic for the CT interactions^[38,41] (Figure S24 in the Supporting Information). The titration curves are satisfactorily fitted with a 1:1 association model and yield apparent stability constants of the order 10^6M^{-1} for both pseudorotaxanes, which are in agreement with the results previously obtained for similar systems.^[38,40,52]

Also the energy ($\lambda_{\text{max}}\approx 460$ nm) and the intensity ($\epsilon_{\text{max}}\approx 500\text{M}^{-1}\text{cm}^{-1}$) of the CT absorption band exhibited by these pseudorotaxanes are consistent with those of similar compounds previously investigated.^[38]

The OH end group of pseudorotaxanes $\text{P}[\mathbf{1}\text{D}2]_{\text{up}}$ and $\text{P}[\mathbf{1}\text{D}3]_{\text{up}}$ was then replaced by the bulky diphenylacetyl moiety by submitting the pseudorotaxanes to the stoppering reaction with diphenylacetyl chloride in toluene (Scheme 3). Compounds $\text{R}[\mathbf{1}\text{D}4]_{\text{up}}$ and $\text{R}[\mathbf{1}\text{D}5]_{\text{up}}$ were obtained and after separation from the reaction mixture they were fully characterized (Figures S14–S22 in the Supporting Information). NMR analysis confirms that in their structure the stilbene-based group is still positioned at the upper rim of the wheel. In the case of $\text{R}[\mathbf{1}\text{D}4]_{\text{up}}$ the exact orientation of its axle with respect to the wheel rims was further confirmed by comparison with the structure of compound $\text{R}[\mathbf{1}\text{D}4]_{\text{down}}$, which was however obtained by threading wheel **1** with axle **4** in benzene by heating to reflux (Scheme 4). The outcome of this threading process gave a mixture of both isomers $\text{R}[\mathbf{1}\text{D}4]_{\text{up}}$ and $\text{R}[\mathbf{1}\text{D}4]_{\text{down}}$ in which the latter was the main isomer ($\approx 90\%$). The presence of the up isomer was verified by 2D NMR experiments (see the Supporting Information). The down isomer was also prepared to verify whether the stilbene units can pass through the calix[6]arene annulus.

Besides the NMR analysis, compounds $\text{R}[\mathbf{1}\text{D}4]_{\text{up}}$ and $\text{R}[\mathbf{1}\text{D}5]_{\text{up}}$ were also characterized by UV/Vis absorption spectroscopy in air-equilibrated CH_2Cl_2 solution at room temperature. Their absorption spectra (Figure 4) show for $\lambda < 350$ nm two bands that, by comparison with the separated molecular components, can be attributed as follows: the intense band with maximum at around $\lambda=260$ nm is as-

Scheme 4. Synthesis of compound R[1D4]_{down}.Figure 4. Absorption spectra (CH_2Cl_2 , RT) of compounds R[1D4]_{up} (solid line) and R[1D5]_{up} (dashed line). The inset shows an enlarged view of the charge-transfer absorption bands.

signed to the absorption of the wheel component and the 4,4'-bipyridinium unit contained in the axle components, whereas the slightly structured band at around $\lambda = 320$ nm is ascribed to the stilbene-type end group of the axles.

The spectra of R[1D4]_{up} and R[1D5]_{up} also show a weak, broad band with a maximum at around $\lambda = 460$ nm that is not present in the spectra of the molecular components and is responsible for the red color (Figure 4, inset). As already discussed in the case of P[1D2]_{up} and P[1D3]_{up}, this visible band can be ascribed to CT interactions between the electron-rich aromatic rings of the wheel and the electron-poor 4,4'-bipyridinium unit contained in the axles. Specifically, the visible absorption bands of the examined compounds are very similar, as far as energy and intensity are concerned, to those of rotaxanes containing wheel 1 and 4,4'-bipyridinium-based dumbbells carrying at both ends a diphenyl-

ylacetyl group.^[40] Compounds R[1D4]_{up} and R[1D5]_{up} exhibit indeed a rotaxane-like behavior because one end of their axle is totally stoppered by the presence of the bulky diphenylacetyl moiety and dethreading from the side carrying the stilbene-type unit is prevented due to kinetic reasons. Their rotaxane-like character is clearly evidenced by the fact that the molar absorption coefficients of the CT absorption band are unaffected by the concentration.

Dethreading of compounds R[1D4]_{up} and R[1D5]_{up}: As already mentioned, in apolar solvents compounds R[1D4]_{up} and R[1D5]_{up} are mainly stabilized by 1) CT interactions between the aromatic rings of the wheel and the bipyridinium ion contained in the axles, 2) hydrogen bonding between the counter anions of the axles and the ureidic groups of the wheel, and 3) solvophobic effects on account of the low solubility of the bipyridinium salts in apolar solvents. These interactions are substantially weakened in polar solvents and, therefore, it is expected that dissolution of compounds R[1D4]_{up} and R[1D5]_{up} in such kind of solvents induces axle dethreading. Because of the presence of the diphenylacetyl stopper at one end of the axles, it is also expected that dethreading occurs by involving the other end side, that is, through the slippage of the sufficiently slim stilbene-type unit from the lower rim of the wheel.

Dethreading of R[1D4]_{up} and R[1D5]_{up} in the polar solvent DMSO was indeed verified through NMR measurements, which clearly show the presence of the axle and wheel as separate components in solution (Figure 5). Substantial insight into the dethreading process was obtained by monitoring the CT absorption band at around $\lambda = 460$ nm over time, which is characteristic of the assembled structure, after dissolution of R[1D4]_{up} and R[1D5]_{up} in DMSO. For both compounds the intensity of this band decreases with time (Figure 6a for R[1D4]_{up} and Figure S23 in the Supporting Information for R[1D5]_{up}); the decrease is faster for R[1D4]_{up} than for R[1D5]_{up}. The absorption spectra observed when the time-dependent changes are over coincide with the sum of the spectra of the respective separated components. This finding is fully consistent with the dethreading of the compounds caused by the solvent-induced weakening of the intercomponent interactions.

Data fitting^[53] shows that the absorbance decays at $\lambda = 460$ nm take place with a first-order kinetic law and with rate constants of 5.9×10^{-3} and $9.3 \times 10^{-5} \text{ s}^{-1}$ for R[1D4]_{up} (Figure 6b, full circles) and R[1D5]_{up} (Figure 7, full circles), respectively. The fact that the rate constants depend on the stilbene structure (unsubstituted and *t*Bu-substituted) is a clear evidence that dethreading occurs through the slippage of this group from the lower rim of the wheel. The two orders of magnitude lower rate constant of R[1D5]_{up} compared with R[1D4]_{up} can indeed be explained on the basis of the higher hampering effect of the *t*Bu-substituted stilbene present in axle 5 compared with the unsubstituted one comprised in axle 4.

Further proofs of these dethreading mode and direction are given by comparison with the behavior of the pseudo-

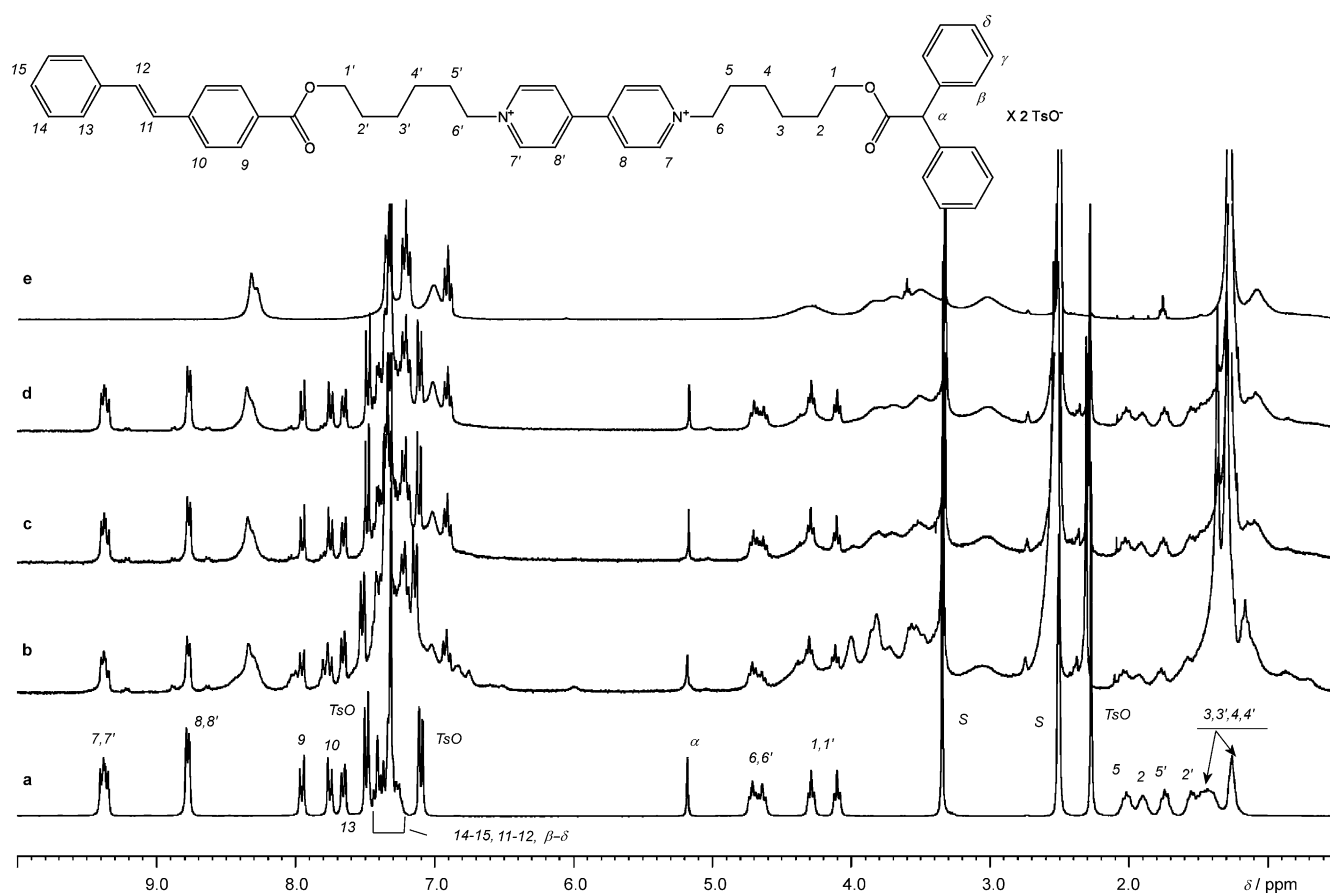


Figure 5. ^1H NMR spectra (300 MHz, $[\text{D}_6]\text{DMSO}$) of a) axle **4**, compound $\text{R}[\text{1D4}]_{\text{up}}$ b) **5**, c) **10**, and d) 30 min after dissolution, and e) wheel **1**. The most diagnostic resonances of axle **4** have been numbered according to the formula placed above the stacked plot.

taxanes $\text{P}[\text{1D2}]_{\text{up}}$ and $\text{P}[\text{1D3}]_{\text{up}}$, and of rotaxanes formed by dumbbells carrying the diphenylacetyl group at both ends. As expected, dissolution of $\text{P}[\text{1D2}]_{\text{up}}$ and $\text{P}[\text{1D3}]_{\text{up}}$ in DMSO causes their quantitative and fast dethreading. Indeed, the absorption spectra of such solutions, monitored immediately after dissolution (within 30 s), do not show any CT band, indicating that disassembly occurs on a timescale faster than that required for dissolution; in other words, the dethreading rate constant is $>0.1 \text{ s}^{-1}$. This value, much higher than that observed for $\text{R}[\text{1D4}]_{\text{up}}$ and $\text{R}[\text{1D5}]_{\text{up}}$, indicates that for the pseudorotaxanes a different dethreading mechanism operates, that is, axles **2** and **3** dethread with the side carrying the OH group from the upper rim of the wheel, that means in a direction opposite to that of the threading. Conversely, the rotaxanes containing dumbbells stoppered by the diphenylacetyl group at both ends do not undergo any structural changes in DMSO, as evidenced by the fact that in this solvent their CT absorption bands are still present and do not change over time. This finding is consistent with the fact that the diphenylacetyl moiety is too bulky to pass through the rims of the wheel.

Photocontrol of the dethreading rate in $\text{R}[\text{1D4}]_{\text{up}}$ and $\text{R}[\text{1D5}]_{\text{up}}$: To further support the involvement of the stil-

bene-type unit in the dethreading process, and investigate the possibility of photocontrolling the dethreading rate, compounds $\text{R}[\text{1D4}]_{\text{up}}$ and $\text{R}[\text{1D5}]_{\text{up}}$ were irradiated in CH_2Cl_2 solution with $\lambda=334$ or 313 nm to induce the *E*-*Z* isomerization of the stilbene end group of the axle (see Figure S25 in the Supporting Information). The photoreaction did not cause any change in the CT absorption band, suggesting that the configuration of the stilbene unit does not affect the inclusion of the 4,4'-bipyridinium ion inside the wheel. Only the band in the $\lambda=300\text{--}350 \text{ nm}$ region, characteristic for the stilbene unit, is affected, as also evidenced by irradiation carried out on separate axles **4** and **5**. For both compound $\text{R}[\text{1D4}]_{\text{up}}$ and $\text{R}[\text{1D5}]_{\text{up}}$ we found that an irradiation of 90 min causes about 70% conversion of the stilbene unit from the *E* to the *Z* isomer.^[54-56] After evaporation of CH_2Cl_2 and addition of DMSO, the CT absorption bands of $\text{R}[\text{1D4}]_{\text{up}}$ and $\text{R}[\text{1D5}]_{\text{up}}$ were monitored. For the photoisomerized compounds, as already observed for the non-irradiated ones, the CT band decreases over time indicating the occurrence of axle dethreading.

In the case of $\text{R}[\text{1D4}]_{\text{up}}$ the best fitting of the absorption values at $\lambda=460 \text{ nm}$ clearly evidences that the disappearance of CT band occurs according to two superimposed first-order kinetics (Figure 6b, open circles) with rate con-

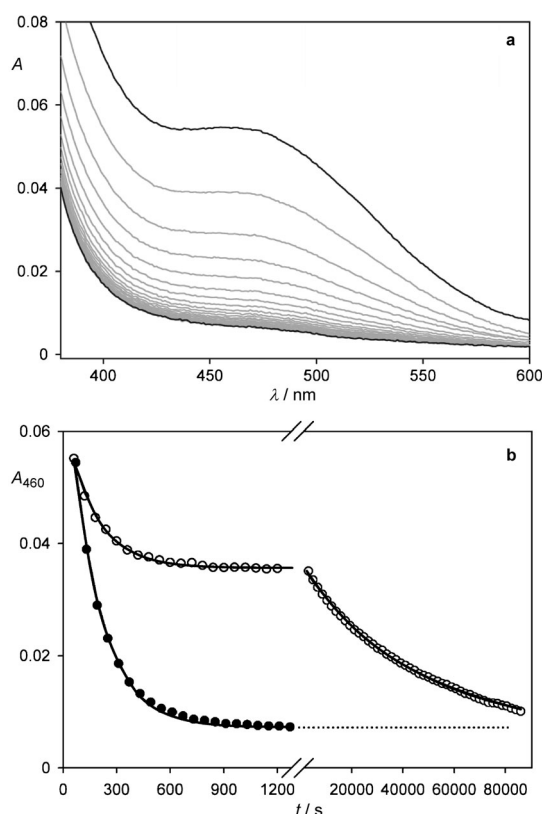


Figure 6. a) Decrease of the CT absorption band of compound $R[1D4]_{up}$ ($2.2 \times 10^{-4} M$) after dissolution in DMSO at RT. b) Absorbance decrease at $\lambda = 460$ nm upon dissolution in of $R[1D4]_{up}$ DMSO before (full circles) and after (open circles) exhaustive irradiation at $\lambda = 334$ nm. The first-order fitting curves are also shown.

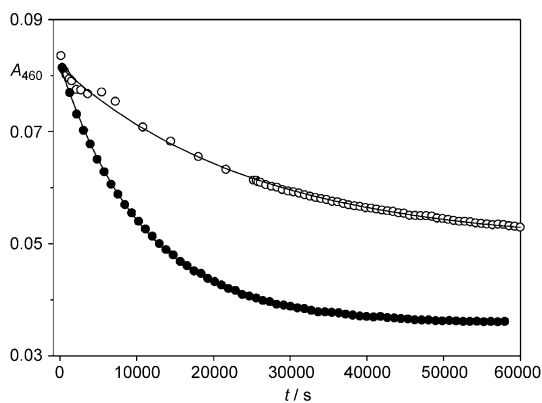


Figure 7. Absorbance decrease at $\lambda = 460$ nm upon dissolution of $R[1D5]_{up}$ in DMSO ($2.3 \times 10^{-4} M$) before (full circles) and after (open circles) exhaustive irradiation at $\lambda = 313$ nm. The first-order fitting curves are also shown.

stants of 5.9×10^{-3} and $2.3 \times 10^{-5} s^{-1}$, respectively. The faster process, which accounts for 30% of the total decay, is attributed to the dethreading of the axle carrying the stilbene *E* isomer because its rate constant coincides with the one obtained for non-irradiated $R[1D4]_{up}$. Consequently, the slower process can be assigned to the dethreading of the axle comprising a *Z* stilbene. The low value of its rate constant is in

agreement with the higher hampering effect of the *Z* isomer compared with the *E* isomer, which results in a much more difficult slippage of this unit through the lower rim of the wheel. It is interesting to notice that the *E*-*Z* photoisomerization affects the dethreading rate constant more than the incorporation of the *tert*-butyl group on the stilbene unit. The rate constant observed upon isomerization is indeed about one order of magnitude slower than that observed in the case of the substituted stilbene.

In the case of $R[1D5]_{up}$ a decrease of the CT absorption band of only about 30% is observed. The best fitting of the absorption values at $\lambda = 460$ nm (Figure 7, open circles) evidences that this decrease occurs according to a first-order kinetics with a rate constant of $4 \times 10^{-5} s^{-1}$, which is quite similar to that obtained for the dethreading of the non-irradiated $R[1D5]_{up}$. We can conclude that the observed decay of the CT absorption band concerns the portion of the compound with the axle carrying the *E* isomer of the *t*Bu stilbene, and that the photoisomerized compound does not undergo dethreading, accounting for the 70% of the CT absorption intensity that does not disappear in DMSO. Hence, our results show that the *Z* isomer of the *t*Bu stilbene is too bulky to pass through the lower rim of the wheel, and that $R[1D5]_{up}$ in its *Z* configuration behaves as a real rotaxane.

Unidirectional transit of the axle through the wheel: Taken together the experiments reported here show that the strategy we developed enables to obtain the unidirectional transit of a molecular axle through a molecular wheel. Our strategy is based on the use of appropriately designed molecular components, an essential feature of which is their nonsymmetric structure, and exploits the following steps.

- 1) In apolar solvents axle **2** or **3** threads into wheel **1** from its upper rim and with the end carrying the -H group. An oriented pseudorotaxane structure is obtained in which the OH group is positioned at the lower rim of the wheel. This threading mode experiences an energetic barrier substantially lower than that of the stilbene threading because of the small hampering effect of the OH group (Figure 8a).
- 2) The stoppering reaction of the obtained pseudorotaxane replaces the small OH group with a bulky diphenylacetyl moiety. This reaction converts the pseudorotaxane in a rotaxane-like species because one end of the axle carries the diphenylacetyl stopper and the other end terminates with the stilbene-type unit that prevents dethreading for kinetic reasons (Figure 8b).
- 3) Replacement of the apolar solvent with the polar solvent DMSO weakens the interactions that stabilize the assembled structure. Such a destabilization substantially lowers the energy barrier associated with the slippage of the stilbene unit and induces the axle dethreading from the lower rim of the wheel (Figure 8c), that is, in the same direction of the axle threading. The complete unidirectional transit of the axle through the wheel is, therefore, accomplished.

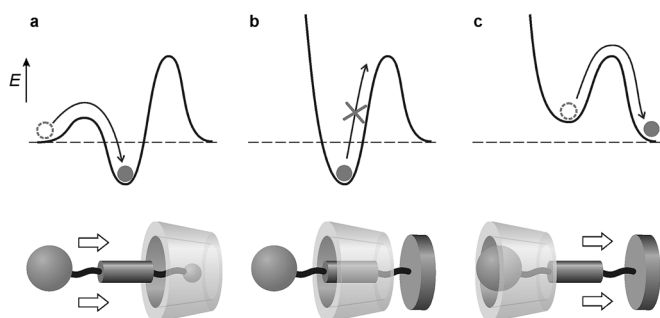


Figure 8. Simplified potential energy curves representing the steps that account for the unidirectional transit of the axle through the wheel. The horizontal coordinate of the diagrams represents the axle–wheel distance when they approach one another along the direction and with the orientation shown in the cartoons. a) Threading of the axle through the upper rim of the wheel in apolar solvents. b) The stoppering reaction to convert the pseudorotaxane into a rotaxane-like species. c) Dethreading of the axle from the lower rim of the wheel occurring in polar solvents.

Conclusion

Although our purpose was not to develop a system of practical use, it should be noted that the experiments described here have several drawbacks. First of all, the chemical reactions and the solvent replacement, which is necessary to obtain the unidirectional transit, make the overall switch procedure rather unpractical, and lead to the accumulation of chemical debris. Full reset and cycling of the system is possible, at least in principle, upon detachment of the diphenylacetate stopper from the axle and re-dissolution of the latter, together with the wheel, in an apolar solvent. In compounds **2** and **3** such a selective de-stoppering is prevented by the nearly identical reactivity of the ester linkages at the two ends of the axles. All these limitations, however, could be removed with a more careful design of the axle component. Finally, it is important to stress the essential role played by the stilbene unit incorporated at one end of the axle. It indeed enables 1) to achieve the unidirectional transit of the axle through the wheel, because its dimensions are not too big to prevent slippage through the wheel, but big enough to induce a kinetic control of the axle threading/dethreading processes and 2) to tune the dethreading rate because of the possibility to modify its hampering effect upon the use of stilbene unit substituted with relatively bulky groups, or, more interesting, upon photoisomerization.

Experimental Section

Materials and synthetic methods: Toluene and dichloromethane were dried by using standard procedure, all other reagents were of reagent grade quality obtained from commercial suppliers and were used without further purification. NMR spectra were recorded at 400 and 300 MHz for ^1H and 100 and 75 MHz for ^{13}C . Melting points are uncorrected. Chemical shifts are expressed in [ppm] (δ) by using the residual solvent signal as internal reference. Mass spectra were recorded in ESI mode. Calix[6]arene (**1**),^[37] (*E*)-4-styrylbenzoic acid (**8a**),^[57] 6-hydroxyhexyl tosylate (**10**),^[58] and 6-(tosyloxy)hexyl 2,2-diphenylacetate (**13**),^[41] were synthesized according to literature procedures.

ylate (**10**),^[58] and 6-(tosyloxy)hexyl 2,2-diphenylacetate (**13**),^[41] were synthesized according to literature procedures.

(*E*)-4-(4-*tert*-Butylstyryl)benzoic acid (8b**):** To a stirred solution of DMF (250 mL) kept under argon atmosphere, 4-bromo benzoic acid (**7**) (1 g, 4.97 mmol), Pd(OAc)₂ (cat.), 1-*tert*-butyl-4-vinylbenzene (**6b**) (1.2 g, 7.5 mmol), K₂CO₃ (1.4 g, 10 mmol), *N,N*-dimethyl- β -alanine (cat.) were added. The resulting heterogeneous mixture was heated to reflux for 6 h. After this period, the reaction mixture was cooled to room temperature, diluted with water (100 mL), and extracted with diethyl ether (2 \times 100 mL). The organic phase was separated, dried with Na₂SO₄, and evaporated under reduced pressure. The orange oily residue was taken up with ethyl acetate and the desired product **8b** was precipitated as a white solid (1 g, 71 %) by addition of *n*-hexane. M.p. 296.0–297.1 °C; ^1H NMR (300 MHz, CDCl₃/CD₃OD 1:1): δ = 7.96 (d, *J* = 8 Hz, 2H), 7.49 (d, *J* = 8 Hz, 2H), 7.42 (d, *J* = 8 Hz, 2H), 7.33 (d, *J* = 8 Hz, 2H), 7.15 (d, *J* = 16 Hz, 1H), 7.03 (d, *J* = 16 Hz, 1H), 1.27 ppm (s, 9H); ^{13}C NMR (75 MHz, CDCl₃/CD₃OD 1:1): δ = 151.4, 146.1, 142.0, 133.8, 130.9, 130.2, 128.7, 126.7, 126.4, 126.0, 125.6, 77.2, 31.1 ppm; MS (ESI): *m/z* (%): 279 (100) [*M*–H][–].

General procedure for the synthesis of compounds 11a and 11b: In a 100 mL round-bottomed flask, the appropriate stilbene derivate **8a** or **8b** (4.5 mmol) and oxalyl chloride (13.4 mmol) were dissolved in dry CHCl₃ (40 mL). The resulting solution was heated to reflux for two hours under a nitrogen atmosphere, then the solvent was evaporated under reduced pressure. The yellow solid residue of the acylic chloride (**9a** or **9b**) was dissolved in dry CH₂Cl₂ (50 mL). To the resulting solution, 6-hydroxyhexyl tosylate (**10**) (1.8 g, 6.7 mmol), triethyl amine (0.68 g, 6.7 mmol) and DMAP (cat.) were added. The reaction mixture was stirred at room temperature for 72 h, then the reaction was quenched by addition of water (50 mL). The separated organic phase was extracted with a saturated solution of NaHCO₃ in H₂O (2 \times 20 mL). After evaporation of the solvent under reduced pressure, the oily residue was purified by column chromatography (hexane/ethyl acetate 8:2).

Compound **11a** was isolated as a white solid (1.2 g, 56 %). M.p. 69–71 °C; ^1H NMR (300 MHz, CDCl₃): δ = 8.01 (d, *J* = 8 Hz, 2H), 7.79 (d, *J* = 8 Hz, 2H), 7.57–7.52 (m, 4H), 7.4–7.3 (m, 5H), 7.22 (d, *J* = 17 Hz, 1H), 7.12 (d, *J* = 17 Hz, 1H), 4.27 (t, *J* = 6.5 Hz, 2H), 4.03 (t, *J* = 6.5 Hz, 2H), 2.43 (s, 3H), 1.8–1.7 (m, 4H), 1.45–1.35 ppm (m, 4H); ^{13}C NMR (75 MHz, CDCl₃): δ = 166.3, 144.6, 141.7, 136.6, 133.1, 131.1, 129.9, 129.7, 129.1, 128.7, 127.8, 127.5, 126.7, 126.2, 70.3, 64.6, 28.7, 28.5, 25.4, 25.0, 21.6 ppm; MS (ESI): *m/z* (%): 501 (50) [*M*+Na]⁺, 517 (25) [*M*+K]⁺.

Compound **11b** was isolated as colorless oil (1.42 g, 60 %). ^1H NMR (300 MHz, CDCl₃): δ = 8.01 (d, *J* = 8 Hz, 2H), 7.78 (d, *J* = 8 Hz, 2H), 7.55 (d, *J* = 8 Hz, 2H), 7.47 (d, *J* = 8 Hz, 2H), 7.39 (d, *J* = 8 Hz, 2H), 7.33 (d, *J* = 8 Hz, 2H), 7.20 (d, *J* = 16 Hz, 1H), 7.10 (d, *J* = 16 Hz, 1H), 4.27 (t, *J* = 6.6 Hz, 2H), 4.03 (t, *J* = 6.5 Hz, 2H), 2.44 (s, 3H), 1.75–1.50 (m, 6H) 1.4–1.3 ppm (m, 11H); ^{13}C NMR (75 MHz, CDCl₃): δ = 166.4, 151.4, 144.6, 142.0, 133.9, 133.1, 131.0, 129.9, 129.8, 128.8, 127.8, 126.7, 126.5, 126.1, 125.7, 70.3, 64.6, 34.6, 31.2, 28.7, 28.4, 25.4, 25.1, 21.6 ppm; MS (ES): *m/z* (%): 557 (40) [*M*+Na]⁺, 573 (15) [*M*+K]⁺.

General procedure for the synthesis of compounds 12a and 12b: 4,4'-Bipyridine (1.2 g, 7.7 mmol) and the appropriate stilbenic derivative **11a** or **11b** (2.5 mmol) were dissolved in CH₃CN (50 mL). The resulting solution was heated to reflux for 72 h, then the solvent was evaporated to dryness under reduced pressure. The desired products were isolated by treating the yellowish oily residue with hot ethyl acetate (2 \times 25 mL) followed by suction filtration.

Compound **12a** was isolated as a white solid (0.8 g, 52 %). M.p. 189.0–191.2 °C; ^1H NMR (300 MHz, CD₃OD): δ = 9.16 (d, *J* = 6.5 Hz, 2H), 8.90 (d, *J* = 6.5 Hz, 2H), 8.51 (d, *J* = 6.5 Hz, 2H), 8.18 (d, *J* = 8 Hz, 2H), 7.95 (d, *J* = 8.1 Hz, 2H), 7.7–7.6 (m, 6H), 7.4–7.2 (m, 8H), 4.70 (t, *J* = 7 Hz, 2H), 4.33 (t, *J* = 7 Hz, 2H), 2.34 (s, 3H), 2.10 (t, *J* = 7 Hz, 2H), 1.82 (t, *J* = 7 Hz, 2H), 1.65–1.31 ppm (m, 4H); ^{13}C NMR (75 MHz, CD₃OD): δ = 166.6, 152.5, 148.2, 145.1, 144.2, 141.9, 140.1, 136.4, 131.2, 129.6, 128.5, 128.4, 128.0, 127.2, 127.0, 126.4, 126.2, 126.1, 125.4, 123.1, 64.4, 61.5, 31.0, 29.3, 28.1, 25.4, 25.1, 20.7 ppm; MS (ESI): *m/z* (%): 463 (100) [*M*–TsO]⁺ (Ts = tosyl).

Compound **12b** was isolated as a white solid (1.3 g, 77%). M.p. 171.8–173.8°C; ¹H NMR (300 MHz, CDCl₃): δ = 9.29 (d, *J* = 6.5 Hz, 2H), 8.74 (d, *J* = 6.5 Hz, 2H), 8.18 (d, *J* = 6.5 Hz, 2H), 7.94 (d, *J* = 8 Hz, 2H), 7.73 (d, *J* = 8 Hz, 2H), 7.57 (d, *J* = 6 Hz, 2H), 7.51 (d, *J* = 8 Hz, 2H), 7.45 (d, *J* = 8 Hz, 2H), 7.38 (d, *J* = 8 Hz, 2H), 7.17 (d, *J* = 16.5 Hz, 2H), 7.08 (d, *J* = 6 Hz, 2H), 7.04 (d, *J* = 16.5 Hz, 2H), 4.77 (d, *J* = 7 Hz, 2H), 4.20 (d, *J* = 7 Hz, 2H), 2.23 (s, 3H), 1.94 (d, *J* = 7 Hz, 2H), 1.64 (d, *J* = 7 Hz, 2H), 1.31 ppm (brs, 13H); ¹³C NMR (75 MHz, CD₃OD): δ = 166.6, 154.1, 151.7, 145.9, 142.4, 141.3, 139.7, 134.3, 131.4, 130.2, 129.0, 126.8, 126.5, 126.2, 126.1, 121.9, 64.9, 62.1, 34.9, 31.8, 31.2, 28.7, 26.0, 25.9, 21.3 ppm; MS (ESI): *m/z* (%): 519 (100) [*M*-TsO]⁺.

General procedure for the synthesis of axles 2 and 3: 6-Hydroxyhexyl tosylate (**10**) (0.3 g, 1.1 mmol) and the appropriate salt **12a** and **12b** (0.7 mmol) were dissolved in CH₃CN (50 mL). The resulting reaction mixture was heated to reflux for ten days and then cooled to room temperature. The solvent was evaporated to dryness under reduced pressure and the crude yellowish solid residue was triturated with hot ethyl acetate (2 × 25 mL). After decantation of the ethyl acetate, the desired axles **2** and **3** were purified by recrystallization from CH₃CN.

Compound **2** was isolated as a white solid (0.45 g, 70%). M.p. 127.0–128.2°C; ¹H NMR (300 MHz, CD₃OD): δ = 9.21–9.17 (m, 4H), 8.60 (d, *J* = 6.5 Hz, 4H), 7.95 (d, *J* = 8.5 Hz, 2H), 7.67 (d, *J* = 8.5 Hz, 2H), 7.63 (d, *J* = 8.5 Hz, 2H), 7.56 (d, *J* = 7.5 Hz, 2H), 7.39–7.27 (m, 5H), 7.19 (d, *J* = 8 Hz, 6H), 4.7–4.6 (m, 4H), 4.30 (t, *J* = 6.5 Hz, 2H), 3.54 (t, *J* = 6.5 Hz, 2H), 2.33 (s, 6H), 2.1 (brs, 4H), 1.8 (brs, 2H), 1.6–1.3 ppm (m, 10H); ¹³C NMR (100 MHz, CD₃OD): δ = 172.9, 166.6, 149.7, 145.6, 142.3, 140.3, 138.9, 136.8, 131.3, 129.6, 128.7, 128.6, 128.4, 128.2, 128.0, 126.9, 126.6, 126.2, 125.6, 64.5, 61.8, 56.9, 30.9, 30.8, 27.9, 25.4, 25.2, 24.8, 21.1, 20.0 ppm; MS (ESI): *m/z* (%): 281 (50) [*M*-2TsO]²⁺.

Compound **3** was isolated as a white solid (0.47 g, 70%). M.p. 131.3–132.8°C; ¹H NMR (300 MHz, CD₃OD): δ = 9.2 (brs, 4H), 8.6 (brs, 4H), 7.93 (d, *J* = 8.3 Hz, 2H), 7.67 (d, *J* = 8.3 Hz, 2H), 7.60 (d, *J* = 8.3 Hz, 2H), 7.49 (d, *J* = 8.3 Hz, 2H), 7.39 (d, *J* = 8.3 Hz, 2H), 7.2–7.1 (m, 6H), 4.8–4.6 (m, 4H), 4.30 (t, *J* = 6 Hz, 2H), 3.54 (t, *J* = 6 Hz, 2H), 2.33 (s, 6H), 2.1 (brs, 4H), 1.8 (brs, 2H), 1.7–1.4 (m, 10H), 1.31 ppm (s, 9H); ¹³C NMR (75 MHz, CD₃OD): δ = 170.4, 155.2, 153.6, 149.5, 147.0, 146.3, 144.2, 137.9, 134.9, 133.41, 132.37, 130.7, 130.2, 130.0, 129.9, 129.4, 129.2, 68.3, 65.6, 65.1, 37.9, 35.7, 34.9, 34.8, 34.2, 31.9, 29.4, 29.3, 29.1, 28.8, 23.8 ppm; MS (ESI): *m/z* (%): 986 (15) [*M*+Na]⁺, 791 (30) [*M*-TsO]⁺, 310 (100) [*M*-2TsO]²⁺.

General procedure for the synthesis of dumbbells 4 and 5: The same procedure as employed for the synthesis of compounds **2** and **3** but by using 6-(tosyloxy)hexyl 2,2-diphenylacetate (**13**) (1.1 mmol) as alkylating agent.

Compound **4** was isolated as a white solid (0.57 g, 75%). M.p. 172.5–173.5°C; ¹H NMR (300 MHz, [D₆]DMSO): δ = 9.24 (d, *J* = 7 Hz, 2H), 9.19 (d, *J* = 7 Hz, 2H), 8.62 (d, *J* = 6 Hz, 4H), 7.98 (d, *J* = 8.5 Hz, 2H), 7.8–7.5 (m, *J* = 8.5 Hz, 8H), 7.4–7.2 (m, 17H), 5.08 (s, 1H), 4.73 (t, *J* = 7.5 Hz, 2H), 4.63 (t, *J* = 7.5 Hz, 2H), 4.32 (t, *J* = 6.5 Hz, 2H), 4.14 (t, *J* = 6.5 Hz, 2H), 2.34 (s, 6H), 2.2–2.1 (m, 2H), 2.1–2.0 (m, 2H), 1.9–1.8 (m, 2H), 1.7–1.5 (m, 6H), 1.3 ppm (brs, 4H); ¹³C NMR (75 MHz, [D₆]DMSO): δ = 168.2, 151.5, 147.3, 144.2, 142.1, 140.7, 138.7, 132.9, 131.2, 130.4, 130.2, 130.0, 129.9, 129.6, 128.6, 128.5, 128.2, 127.8, 127.2, 66.1, 63.5, 64.4, 58.5, 32.6, 32.5, 29.8, 29.5, 27.1, 26.9, 26.8, 26.5, 21.6 ppm; MS (ESI): *m/z* (%) 379.1 (100) [*M*-2TsO]²⁺, 929 (15) [*M*-TsO]⁺.

Compound **5** was isolated as a white solid (0.56 g, 70%). M.p. 176.5–177.5°C; ¹H NMR (300 MHz, CD₃OD): δ = 9.22 (d, *J* = 8 Hz, 2H), 9.17 (d, *J* = 8 Hz, 2H), 8.60 (d, *J* = 6.5 Hz, 2H), 7.95 (d, *J* = 8 Hz, 2H), 7.67 (d, *J* = 8 Hz, 4H), 7.62 (d, *J* = 8 Hz, 2H), 7.51 (d, *J* = 8 Hz, 2H), 7.41 (d, *J* = 8 Hz, 2H), 7.3–7.1 (m, 16H), 5.05 (s, 1H), 4.73 (t, *J* = 7.5 Hz, 2H), 4.62 (t, *J* = 7.5 Hz, 2H), 4.31 (t, *J* = 6.5 Hz, 2H), 4.13 (t, *J* = 6.5 Hz, 2H), 2.33 (s, 6H), 2.12–2.08 (m, 2H), 2.02–1.96 (m, 2H), 1.81 (t, *J* = 7 Hz, 2H), 1.7–1.5 (m, 6H), 1.32 ppm (s, 9H); ¹³C NMR (75 MHz, CD₃OD): δ = 171.9, 165.9, 147.3, 142.0, 132.7, 131.2, 130.1, 129.9, 129.8, 128.0, 127.7, 127.2, 127.0, 66.1, 63.4, 58.5, 32.6, 32.5, 31.9, 29.9, 29.5, 27.1, 26.9, 26.8, 26.5, 21.6 ppm; MS (ESI): *m/z* (%) 407.4 (100) [*M*-2TsO]²⁺.

General procedure for synthesis of P[1↔2]_{up} and P[1↔3]_{up}: In a round-bottomed flask, the proper amount of the axle (**2** or **3**) (0.05 mmol) was suspended in a solution of compound **1** (0.06 g, 0.04 mmol) in C₆D₆

(4 mL). After stirring at RT for 2 h, the resulting deep-red colored heterogeneous solution was filtered off to remove the excess of axle and submitted to NMR analysis with no further purification.

Compound P[1↔2]_{up}: ¹H NMR (300 MHz, C₆D₆): δ = 9.5 (brs, 6H), 8.44 (d, *J* = 8 Hz, 2H), 8.27 (d, *J* = 8 Hz, 4H), 8.2–7.9 (3 br s, 10H), 7.70 and 7.7–7.5 (s and m overlapped, 9H), 7.42 (d, *J* = 8 Hz, 6H), 7.2–6.8 (m, d, *J* = 8 Hz, m, 26H), 4.66 (d, *J* = 14 Hz, 6H), 4.41 (brt, *J* = 7 Hz, 2H), 4.1–3.3 (s, brs, brs and m, 48H), 2.1–2.0 and 2.06 (brs and s overlapped, 8H), 1.80 and 1.69 (2s, 36H), 1.5–1.1 (2m, 22H), 1.1–0.9 ppm (brs, 6H).

Compound P[1↔3]_{up}: ¹H NMR (300 MHz, C₆D₆): δ = 9.5 (brs, 6H), 8.44 (d, *J* = 7.5 Hz, 2H), 8.26 (brd, *J* = 6 Hz, 4H), 8.2–7.8 (3brs, 10H), 7.8 (brs, 2H), 7.69 (s, 6H), 7.6–7.5 (m, 12H), 7.2–7.1 (m, 12H), 7.03 (d, *J* = 8 Hz, 4H), 7.0–6.7 (m, 7H), 4.66 (d, *J* = 15 Hz, 6H), 4.41 (brs, 2H), 4.1–3.3 (s, brs, brs and m, 48H), 2.2 (brs, 6H), 2.0 (brs, 6H), 1.9–1.5 (2brs, 34H), 1.5, 1.36 and 1.20 (brs, s and brt, *J* = 7 Hz, 38H), 1.1–0.9 ppm (brs, 6H).

General procedure for synthesis of R[1↔4]_{up} and R[1↔5]_{up}: Axle **2** or **3** (0.04 mmol) was suspended in a solution of compound **1** (0.06 g, 0.04 mmol) in dry toluene (10 mL). The resulting heterogeneous mixture was stirred at RT until the solution turned to a deep-red color (2 h). Diphenylacetyl chloride (0.015 g, 0.06 mmol) and triethylamine (0.006 g, 0.06 mmol) were then added. After three days the solvent was completely removed under reduced pressure. The red solid residue was dissolved in CH₂Cl₂ (15 mL) and the solution extracted with an aqueous solution of HCl (10% w/v, 2 × 15 mL). The separated organic phase was extracted with an aqueous solution of NaOTs (2 × 15 mL) to regenerate the TsO⁻ ions. The separated organic phase was then dried with CaCl₂ and evaporated to dryness under reduced pressure.

Compound R[1↔4]_{up}: The red solid residue was triturated with *n*-hexane (3 × 20 mL) to afford 0.06 g of R[1↔4]_{up} (63%) as a red solid. M.p. 121.5–122.8°C; ¹H NMR (300 MHz, C₆D₆): δ = 9.47 (s, 6H), 8.43 (d, *J* = 8.1 Hz, 2H), 8.3 (brs, 4H), 8.2–7.9 (m, 10H), 7.8 (brs, 3H), 7.69 (s, 6H), 7.6–7.5 (m, 13H), 7.45 (d, *J* = 7.3 Hz, 2H), 7.3–7.1 (m, 16H), 7.1–6.9 (m, 5H), 6.8 (brs, 7H), 5.22 (s, 1H), 4.65 (d, *J* = 14.5 Hz, 6H), 4.5–4.4 (m, 4H), 4.0 (brs, 15H), 3.7 (brs, 8H), 3.6–3.4 (m, 14H), 2.2 (brs, 2H), 2.06 (s, 6H) 1.9 (brs, 4H), 1.79 (s, 29H), 1.6 (brs, 2H), 1.40 (s, 9H), 1.4–1.1 (m, 11H), 0.9–0.8 ppm (m, 4H); ¹³C NMR (100 MHz, C₆D₆): δ = 172.1, 166.0, 153.5, 152.8, 148.1, 148.0, 144.4, 142.9, 141.2, 139.5, 139.0, 137.5, 137.1, 133.8, 132.1, 131.0, 130.0, 129.7, 129.3, 128.9, 128.8, 128.6, 128.4, 126.9, 126.5, 125.7, 124.8, 121.2, 118.1, 116.7, 72.4, 69.9, 66.3, 64.5, 61.0, 60.6, 57.3, 34.5, 31.5, 29.8, 29.2, 28.6, 28.3, 26.9, 25.7, 25.2, 20.8, 15.2 ppm; MS (ESI): *m/z* (%): 1112 (100) [*M*-2TsO]²⁺; elemental analysis calcd (%) for C₁₅₅H₁₇₆O₂₂S₂N₈ (2567.25): C 72.52, H 6.91, S 2.50, N 4.36; found: C 72.89, H 7.03, S 2.37, N 4.39.

Compound R[1↔5]_{up}: The red solid residue was triturated with *n*-hexane (3 × 20 mL) to afford 0.06 g of R[1↔5]_{up} (63%). M.p. 146.5–148.0°C; ¹H NMR (300 MHz, C₆D₆): δ = 9.5 (brs, 6H), 8.43 (d, *J* = 8 Hz, 2H), 8.3 (brs, 4H), 8.1–7.9 (m, 10H), 7.8 (brs, 3H), 7.69 (s, 6H), 7.6–7.4 (m, 13H), 7.3–7.1 (m, 13H), 7.04 (brs, 5H), 6.9 (brs, 2H), 6.8 (brs, 5H), 5.22 (s, 1H), 4.65 (d, *J* = 14.5 Hz, 6H), 4.5–4.4 (m, 4H), 4.1–3.9 (brs, 15H), 3.8–3.6 (brs, 8H), 3.6–3.4 (m, 14H), 2.2 (brs, 2H), 2.1 (s, 6H) 1.9 (brs, 4H), 1.79 (s, 29H), 1.6 (brs, 2H), 1.40 (s, 9H), 1.4–1.1 (m, 11H), 0.9 ppm (brs, 4H); ¹³C NMR (100 MHz, C₆D₆): δ = 172.1, 166.0, 153.5, 152.8, 151.0, 148.1, 148.0, 144.3, 143.0, 142.0, 141.0, 139.6, 139.3, 139.0, 137.4, 134.4, 133.8, 132.1, 131.0, 130.0, 129.5, 129.2, 129.1, 129.0, 128.9, 128.7, 128.4, 127.0, 126.9, 126.8, 126.5, 125.7, 124.8, 121.2, 119.6, 119.1, 118.1, 116.7, 72.4, 69.9, 66.3, 64.9, 64.5, 61.0, 60.6, 59.7, 57.3, 57.1, 34.5, 34.3, 34.1, 31.5, 31.0, 29.8, 29.3, 29.2, 28.6, 28.2, 27.7, 26.8, 26.0, 25.2, 20.8, 15.2 ppm; MS (ES): *m/z* (%): 1140 (100) [*M*-2TsO]²⁺; elemental analysis calcd (%) for C₁₅₉H₁₈₈O₂₂S₂N₈ (2623.35): C 72.79, H 7.07, S 2.44, N 4.27; found: C 73.51, H 7.30, S 1.69, N 4.27.

Synthesis of R[1↔4]_{down}: To a solution of wheel **1** (0.013 g, 0.009 mmol) in C₆D₆ (0.6 mL) placed in a 5 mm NMR tube axle **4** (0.01 g, 0.009 mmol) was added. The resulting heterogeneous mixture was heated to 70°C for 12 h until the solution turned homogeneous and deep-red colored and analyzed by ¹H and ¹³C NMR spectroscopy as well as mass spectrometry. ¹H NMR (300 MHz, C₆D₆): δ = 9.5 (brs, 6H), 8.4 (d, *J* = 8 Hz, 2H), 8.28 (d, *J* = 7 Hz, 4H), 8.2 (brs, 2H), 8.1 (brs, 6H), 7.95 (d, *J* = 6.5 Hz, 2H),

7.8 (brs, 6H), 7.69 (s, 6H), 7.46 (d, $J=7$ Hz, 4H), 7.45 (d, $J=7$ Hz, 4H), 7.4–7.2 (m, 8H), 7.2–7.1 (m, 6H), 7.1–7.0 (m, 5H), 6.9 (brs, 4H), 6.78 (t, $J=7$ Hz, 3H), 5.23 (s, 1H), 4.69 (d, $J=14$ Hz, 6H), 4.7 (brs, 2H), 4.13 (t, $J=7$ Hz, 2H), 4.05 (s, 9H), 4.0 (brs, 8H), 3.7 (brs, 8H), 3.6–3.5 (m, 12H), 2.2 (brs, 2H), 2.04 (s, 8H), 1.8 (brs, 31H), 1.4 (brs, 4H), 1.24 (t, $J=7$ Hz, 9H), 1.0 (brs, 2H), 0.9 ppm (brs, 2H); ^{13}C NMR (100 MHz, C_6D_6): $\delta=172.0, 165.9, 153.5, 152.8, 148.1, 148.0, 144.3, 143.2, 143.0, 141.1, 139.4, 139.2, 137.5, 136.7, 133.8, 132.1, 131.6, 130.0, 129.3, 129.0, 128.7, 128.6, 127.2, 126.8, 126.5, 125.6, 125.3, 124.8, 121.2, 118.1, 116.7, 72.4, 70.0, 66.3, 64.7, 61.0, 60.4, 59.7, 57.4, 38.2, 34.6, 31.5, 31.3, 29.8, 29.6, 29.2, 28.3, 25.5, 24.9, 20.7, 15.2, 13.9$ ppm; MS (ESI): m/z (%): 1112 (100) [$M-2\text{TsO}^-$] $^+$.

UV/Vis spectroscopy and photoisomerization experiments: Absorption spectra were recorded by using a Perkin–Elmer $\lambda 45$ or $\lambda 650$ spectrophotometer with air-equilibrated CH_2Cl_2 or DMSO solutions at RT (298 K), with concentrations in the 1×10^{-5} – 1×10^{-3} M range. Solutions were examined in 1 cm spectrofluorimetric quartz cells (wavelength experimental error: ± 1 nm). Photochemical reactions were performed on stirred air-equilibrated CH_2Cl_2 solutions at RT by using a Hanau Q400 medium pressure Hg lamp (150 W). The selection of the desired irradiation wavelength ($\lambda=313$ or 334 nm) was accomplished by the use of an appropriate interference filter.

Acknowledgements

This work was supported by the Italian MIUR (PRIN 2008HZJW2L) and the Universities of Bologna and Parma. We thank CIM (Centro Interdipartimentale di Misura) “G. Casnati” of the University of Parma for NMR spectroscopic measurements.

[1] R. A. L. Jones, *Soft Machines, Nanotechnology and Life*, Oxford University Press, New York, **2004**.
 [2] D. S. Goodsell, *Bionanotechnology—Lessons from Nature*, Wiley, New York, **2004**.
 [3] S. Mann, *Angew. Chem.* **2008**, *120*, 5386–5401; *Angew. Chem. Int. Ed.* **2008**, *47*, 5306–5320.
 [4] T. Kawaguchi, H. Honda, *BioSystems* **2007**, *90*, 253–262.
 [5] P. Xie, S.-X. Dou, P.-Y. Wang, *Biophys. Chem.* **2006**, *122*, 90–100.
 [6] P. L. Anelli, P. R. Ashton, N. Spencer, A. M. Z. Slawin, J. F. Stoddart, D. J. Williams, *Angew. Chem.* **1991**, *103*, 1052–1054; *Angew. Chem. Int. Ed. Engl.* **1991**, *30*, 1036–1039.
 [7] *Catenanes, Rotaxanes, and Knots* (Eds.: J. P. Sauvage, C. Dietrich-Buchecker), Wiley-VCH, Weinheim, **1999**.
 [8] V. Balzani, M. Venturi, A. Credi, *Molecular Devices and Machines—Concepts and Perspectives for the Nanoworld*, 2nd ed., Wiley-VCH, Weinheim, **2008**.
 [9] V. Balzani, A. Credi, M. Venturi, *Proc. Natl. Acad. Sci. USA* **2002**, *99*, 4814–4817.
 [10] S. Saha, K. C. F. Leung, T. D. Nguyen, J. F. Stoddart, J. I. Zink, *Adv. Funct. Mater.* **2007**, *17*, 685–693.
 [11] X. Ma, Q. C. Wang, D. H. Qu, Y. Xu, F. Y. Ji, H. Tian, *Adv. Funct. Mater.* **2007**, *17*, 829–837.
 [12] D. Sobransingh, A. E. Kaifer, *Org. Lett.* **2006**, *8*, 3247–3250.
 [13] S. J. Vella, J. Tiburcio, J. W. Gauld, S. J. Loeb, *Org. Lett.* **2006**, *8*, 3421–3424.
 [14] S. Silvi, A. Arduini, A. Pochini, A. Secchi, M. Tomasulo, F. M. Raymo, M. Baroncini, A. Credi, *J. Am. Chem. Soc.* **2007**, *129*, 13378–13379.
 [15] Y.-L. Huang, W.-C. Hung, C.-C. Lai, Y.-H. Liu, S.-M. Peng, S.-H. Chiu, *Angew. Chem.* **2007**, *119*, 6749–6753; *Angew. Chem. Int. Ed.* **2007**, *46*, 6629–6633.
 [16] D. Tuncel, M. Katterle, *Chem. Eur. J.* **2008**, *14*, 4110–4116.
 [17] J. W. Lee, I. Hwang, W. S. Jeon, Y. H. Ko, S. Sakamoto, K. Yamaguchi, K. Kim, *Chem. Asian J.* **2008**, *3*, 1277–1283.
 [18] J. W. Park, H. J. Song, *Org. Lett.* **2004**, *6*, 4869–4872.

[19] N. Mourtzis, K. Eliadou, K. Yannakopoulou, *Supramol. Chem.* **2004**, *16*, 587–593.
 [20] J. W. Park, *J. Phys. Chem. B* **2006**, *110*, 24915–24922.
 [21] J. W. Park, H. J. Song, H.-J. Chang, *Tetrahedron Lett.* **2006**, *47*, 3831–3834.
 [22] T. Oshikiri, Y. Takashima, H. Yamaguchi, A. Harada, *Chem. Eur. J.* **2007**, *13*, 7091–7098.
 [23] J. W. Park, H. J. Song, Y. J. Cho, K. K. Park, *J. Phys. Chem. C* **2007**, *111*, 18605–18614.
 [24] T. Oshikiri, Y. Takashima, H. Yamaguchi, A. Harada, *J. Am. Chem. Soc.* **2005**, *127*, 12186–12187.
 [25] T. Oshikiri, H. Yamaguchi, Y. Takashima, A. Harada, *Chem. Commun.* **2009**, 5515–5517.
 [26] E. R. Kay, D. A. Leigh, F. Zerbetto, *Angew. Chem.* **2007**, *119*, 72–196; *Angew. Chem. Int. Ed.* **2007**, *46*, 72–191.
 [27] M. N. Chatterjee, E. R. Kay, D. A. Leigh, *J. Am. Chem. Soc.* **2006**, *128*, 4058–4073.
 [28] W. R. Browne, B. L. Feringa, *Nat. Nanotechnol.* **2006**, *1*, 25–35.
 [29] T. R. Kelly, H. de Silva, R. A. Silva, *Nature* **1999**, *401*, 150–152.
 [30] T. R. Kelly, J. P. Sestelo, I. Tellitu, *J. Org. Chem.* **1998**, *63*, 3655–3665.
 [31] W. B. Sherman, N. C. Seeman, *Nano Lett.* **2004**, *4*, 1203–1207.
 [32] F. C. Simmel, *ChemPhysChem* **2009**, *10*, 2593–2597.
 [33] J. Bath, A. J. Turberfield, *Nat. Nanotechnol.* **2007**, *2*, 275–284.
 [34] Special issue on DNA-based nanoarchitectures and nanomachines: *Org. Biomol. Chem.* **2006**, *4*, 3369–3540.
 [35] M. von Delius, E. M. Geertsema, D. A. Leigh, *Nat. Chem.* **2010**, *2*, 96–101.
 [36] *Molecular Motors* (Ed.: M. Schliwa), Wiley-VCH, Weinheim, **2003**.
 [37] A. Arduini, F. Calzavacca, A. Pochini, A. Secchi, *Chem. Eur. J.* **2003**, *9*, 793–799.
 [38] A. Credi, S. Dumas, S. Silvi, M. Venturi, A. Arduini, A. Pochini, A. Secchi, *J. Org. Chem.* **2004**, *69*, 5881–5887.
 [39] A. Arduini, F. Ciesa, M. Fragassi, A. Pochini, A. Secchi, *Angew. Chem.* **2005**, *117*, 282–285; *Angew. Chem. Int. Ed.* **2005**, *44*, 278–281.
 [40] A. Arduini, R. Bussolati, A. Credi, A. Pochini, A. Secchi, S. Silvi, M. Venturi, *Tetrahedron* **2008**, *64*, 8279–8286.
 [41] A. Arduini, R. Bussolati, A. Credi, G. Faimani, S. Garaudee, A. Pochini, A. Secchi, M. Semeraro, S. Silvi, M. Venturi, *Chem. Eur. J.* **2009**, *15*, 3230–3242.
 [42] M. Ménand, A. Leroy, J. Marrot, M. Luhmer, I. Jabin, *Angew. Chem.* **2009**, *121*, 5617–5620; *Angew. Chem. Int. Ed.* **2009**, *48*, 5509–5512.
 [43] J. P. M. van Duynhoven, R. G. Janssen, W. Verboom, S. M. Franken, A. Casnati, A. Pochini, R. Ungaro, J. De Mendoza, P. M. Nieto, P. Prados, D. N. Reinhoudt, *J. Am. Chem. Soc.* **1994**, *116*, 5814–5822.
 [44] P. R. Ashton, I. Baxter, M. C. T. Fyfe, F. M. Raymo, N. Spencer, J. F. Stoddart, A. J. P. White, D. J. Williams, *J. Am. Chem. Soc.* **1998**, *120*, 2297–2307.
 [45] A. Affeld, G. M. Hubner, C. Seel, C. A. Schalley, *Eur. J. Org. Chem.* **2001**, 2877–2890.
 [46] Simple molecular mechanics calculations showed that the stilbene-type unit, for both compounds **2** and **3**, although bulkier than the hexanol chain, when present in the *E* geometry is slim enough to pass through the calixarene annulus of **1**. This suggests that in principle, during the threading phase carried out in apolar media, both axles could thread the wheel with (through) both termini, from the upper rim.
 [47] Q. C. Wang, D. H. Qu, J. Ren, K. C. Chen, H. Tian, *Angew. Chem.* **2004**, *116*, 2715–2719; *Angew. Chem. Int. Ed.* **2004**, *43*, 2661–2665.
 [48] V. Serreli, C.-F. Lee, E. R. Kay, D. A. Leigh, *Nature* **2007**, *445*, 523–527.
 [49] A. Coskun, D. C. Friedman, H. Li, K. Patel, H. A. Khatib, J. F. Stoddart, *J. Am. Chem. Soc.* **2009**, *131*, 2493–2495.
 [50] a) M. Baroncini, S. Silvi, M. Venturi, A. Credi, *Chem. Eur. J.* **2010**, *16*, 11580–11587. b) M. Baroncini, S. Silvi, M. Venturi, A. Credi, *Angew. Chem.* **2012**, *124*, 4299–4302; *Angew. Chem. Int. Ed.* **2012**, *51*, 4223–4226.

- [51] F. Ugozzoli, C. Massera, A. Arduini, A. Pochini, A. Secchi, *Cryst-EngComm* **2004**, *6*, 227–232.
- [52] A. Arduini, A. Credi, G. Faimani, C. Massera, A. Pochini, A. Secchi, M. Semeraro, S. Silvi, F. Ugozzoli, *Chem. Eur. J.* **2008**, *14*, 98–106.
- [53] SPECFIT, Spectrum Software Associates, R. A. Binstead, Chapel Hill, **1996**.
- [54] This percentage of photoisomerization has been evaluated from the kinetic investigations performed on **R[1 \rightarrow 4]up** and **R[1 \rightarrow 5]up** in DMSO; it is also consistent with the results obtained upon photoisomerization of stilbene under comparable experimental conditions (see for example Refs. [55] and [56]).
- [55] J. Saltiel, A. Marinari, D. W.-L. Chang, J. C. Mitchener, E. D. Megarity, *J. Am. Chem. Soc.* **1979**, *101*, 2982–2996.
- [56] *Photochromism: Molecules and Systems* (Eds.: H. Dürr, H. Bouas-Laurent), Elsevier, Amsterdam, **2003**.
- [57] X. Cui, Z. Li, C.-Z. Tao, Y. Xu, J. Li, L. Liu, Q.-X. Guo, *Org. Lett.* **2006**, *8*, 2467–2470.
- [58] A. Bouzide, G. Sauvè, *Org. Lett.* **2002**, *4*, 2329–2332.

Received: May 9, 2012

Revised: August 6, 2012

Published online: October 22, 2012